Applied Catalysis A: General 378 (2010) 144–150

Contents lists available at ScienceDirect

Applied Catalysis A: General

journal homepage: www.elsevier.com/locate/apcata

Effect of V in $La_2Ni_xV_{1-x}O_{4+\delta}$ on selective oxidative dehydrogenation of propane

Salvatore Crapanzano, Igor V. Babich, Leon Lefferts*

Catalytic Processes and Materials, Faculty of Science and Technology, IMPACT, University of Twente, P.O. Box 217, 7500 AE Enschede, The Netherlands

ARTICLE INFO

Article history:
Received 27 October 2009
Received in revised form 3 February 2010
Accepted 9 February 2010
Available online 13 February 2010

Keywords:
Selective oxidative dehydrogenation
Propane
La_2NiO_4
Over-stoichiometric oxygen
Pulse test

ABSTRACT

In this study, non-stoichiometric redox compounds such as $La_2NiO_{4+\delta}$, $La_2Ni_{0.95}V_{0.05}O_{4.07+\delta}$ and $La_2Ni_{0.9}V_{0.1}O_{4.15+\delta}$ have been tested as oxidants in selective oxidation of propane, in order to judge the suitability of these materials for a dense membrane reactor for selective propane oxidation. Reducibility of the samples has been investigated using temperature programmed reduction in H_2/Ar flow. The catalysts' activity and selectivity at 550 °C have been investigated employing sequential pulses of diluted propane over the oxides.

Pulsing with propane induces step-by-step reduction of the oxide; consequently, the activity of remaining oxygen decreases with the number of pulses, affecting the products distribution. It is observed that at 550 °C on oxidized catalysts CO_2 and H_2O are the main products and the selectivity towards propylene is very low. At a certain reduction level, obtained after pulse 8 in our experiments, the production of CO_2 stopped without changing the amount of C_3H_6 produced. At this stage, also CH_4 and C_2H_4 are being formed. V-doped catalysts have shown a constant level of C_3H_6 production within a broad window of oxidation degree, while the performance of $La_2NiO_{4+\delta}$, catalyst deteriorated drastically after just a few pulses. CO, CH_4 and coke deposits are formed with $La_2NiO_{4+\delta}$, caused by the formation of metallic Ni. Vanadium is able to prevent this phenomenon, thus drastically broadening the window of selective oxidation of propane.

© 2010 Elsevier B.V. All rights reserved.

1. Introduction

Selective oxidation of propane to light olefins is an important research subject since the demand of such olefins is growing. In the last few decades many catalytic systems have been investigated for this reaction including alkali salts [1], metal molybdates [2] and metal vanadates [3]. Promising performance of V/MgO was reported, showing 60% selectivity to olefins at 15% propane conversion employing co-feed of gaseous C_3H_8 and O_2 [4,5]. The major challenge in selective catalytic oxidation of alkanes is the fact that the desired products are more reactive than the alkane reactant, causing domination of total combustion especially at high conversion level.

One effective way to minimize deep oxidation is to avoid the direct contact between products and reactants such as molecular gaseous oxygen. This approach can be used in a moving bed reactor [6] or in a catalytic dense membrane reactor (CDMR) [7]. In the last case, the membrane, as physical separator between products and oxygen, defines two separate compartments, where reaction and regeneration occurs respectively. In case of oxidative dehydrogenation of propane, the reactive side of the membrane is depleted in oxygen. Regeneration of the membrane surface at reaction side occurs *via* ionic permeation (O^{2-} and/or O^-) through the membrane body, originated from oxidation of the membrane with molecular oxygen at the regeneration side. At the same time, to counterbalance the permeation of oxygen ions through the membrane body, migration of electrons in opposite direction occurs. Comparable ionic and electronic permeability rates are required to avoid charge accumulation, slowing down the diffusion of oxygen ions. If the reactivity of the surface oxygen and oxygen permeability are matched, continuous operation of the membrane reactor with high selectivity to olefins can be achieved. This would require tuning of the material composition, temperature as well as concentrations of propane and oxygen.

Suitable materials for this purpose are redox mixed metal oxides with a well organized structure, able to provide oxygen ions for oxidation reactions (Mars – Van Krevelen mechanism). Therefore materials such as perovskite and related compounds have been extensively studied for oxidative dehydrogenation of alkanes in CDMR mode. The ideal perovskite structure, indicated as ABO_3, consists on a cubic arrangement of corner-sharing BO_6 octahedra, where B is a transition metal cation. The A-site ions, located in inter-

* Corresponding author. Tel.: +31 534893033; fax: +31 534894683.
E-mail addresses: L.Lefferts@utwente.nl, l.lefferts@tnw.utwente.nl (L. Lefferts).

0926-860X/$ – see front matter © 2010 Elsevier B.V. All rights reserved.
doi:10.1016/j.apcata.2010.02.012

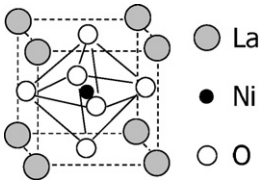

Fig. 1. Schematic representation of perovskite structure.

stitial position between the BO_6 octahedra, are usually occupied by an alkali, alkali earth or rare earth ion [8], as shown in Fig. 1 for $LaNiO_3$.

These materials allow easy redox transformations due to the presence of redox metals (V, Ni, Mo, Bi, Fe). Synthesis conditions, like calcination temperature, partial pressure of oxygen, heating and cooling rate, affect the structure as well as the amount of oxygen in the samples, and consequently the amount of vacant sites.

In the case of $LaNiO_3$, it was shown that under oxidative atmosphere the perovskite structure is stable up to 850 °C [9,10]. Exceeding that temperature, the material reversibly decomposes to NiO and La_2NiO_4, which shows a modified perovskite structure called K_2NiF_4-type structure. In the case of K_2NiF_4 structure, the material possesses a double layer structure: Ni, octahedrally coordinated, is present in the perovskite layer; and La, tetragonally coordinated, is present in a rock-salt layer, as shown in Fig. 2.

Such changes in crystallographic structure obviously influence the thermodynamic activity of oxygen ions in the oxide. In fact, the re-arrangement of the material in the double layer structure enables the formation of "interstitial oxygen" in the inter-layer position. This can bring about oxygen over-stoichiometry. As a result, K_2NiF_4 structure materials have one extra crystallographic type of oxygen ions which might have different thermodynamic activities as compared to strongly bonded lattice oxygen ions. The material is conventionally represented as $La_2NiO_{4+\delta}$, where δ corresponds to the amount of over-stoichiometric interstitial oxygen; Ni^{2+} is partially oxidized to Ni^{3+} in order to compensate for the extra negative charge [11–13].

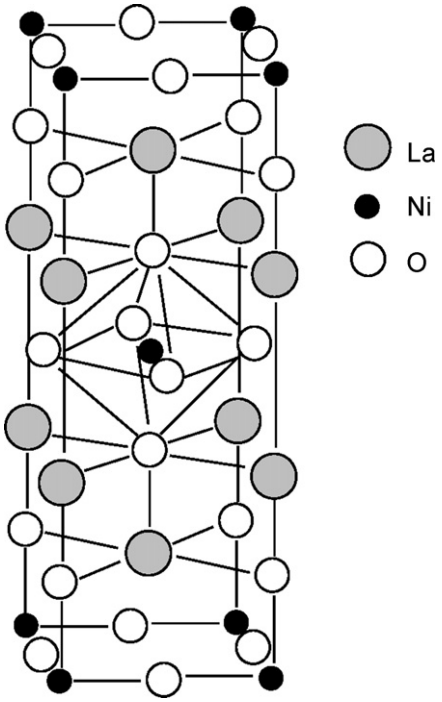

Fig. 2. Schematic representation of K_2NiF_4 structure for La_2NiO_4.

In addition, the chemical and physical properties of K_2NiF_4-type materials can be modified by adding dopants [14]. Structural distortion and variation of activity of oxygen species depend on ionic radius and valency of the dopant [15]. It was reported [16] that structural stability of Eu_2NiO_4 can be increased by adding Sr as dopant. Substitution of Ni^{2+} with V^{5+} in La_2NiO_4 brings extra positive charge to the material, which must be compensated with additional oxygen ions in interstitial positions or in oxygen vacant sites. To the best of our knowledge, the influence of addition of V on the reactivity of O^{2-} ions with propane was not addressed in the literature.

Reactivity of oxygen species can be elucidated from propane pulse experiments. Strictly speaking these are not catalytic experiments; nevertheless, we are using the term catalysts for brevity reasons. During the propane pulses the catalyst provides oxygen ion species to the reaction, increasing the reduction level of the materials with the number of pulses. Oxygen is not present in the gas phase, in contrast to classical co-feed catalytic test with propane and oxygen, and regeneration of the surface sites does not occur during the propane pulses, except for O^{2-} delivery from the bulk of the oxide. The consequent depletion of oxygen active species implies changes in the reactivity of the remaining oxygen species in the catalyst. In this way the influence of the reactivity of the oxygen species on conversion and selectivity can be determined. In addition, reaction pathways which involve gas phase oxygen and adsorbed oxygen are avoided.

In this study the variation of propane conversion and selectivity to olefins as a function of the reduction degree of $La_2Ni_xV_{1-x}O_{4+\delta}$ catalysts is reported. The role of V in enhancing the selectivity towards propylene is discussed.

2. Experimental

2.1. Catalyst preparation

$La_2NiO_{4+\delta}$ (LN), $La_2Ni_{0.95}V_{0.05}O_{4.07+\delta}$ (LNV-05) and $La_2Ni_{0.9}V_{0.1}O_{4.15+\delta}$ (LNV-10) were prepared *via* sol–gel method using EDTA as chelating agent [17]. The appropriate amount of V_2O_5 (Merck) was dissolved in diluted HNO_3 (Merck) at 80 °C under stirring for 1 h. A stoichiometric amount of $La(NO_3)_3{\bullet}6H_2O$ (Merck), $Ni(NO_3)_2{\bullet}6H_2O$ (Merck), EDTA and NH_4OH solutions were added and the obtained solution was heated for 2 h under stirring. After drying at 230 °C, foam-type material was formed and pyrolysis took place after spontaneous ignition. The resulting solid mixed metal oxides were milled and calcined in air, slowly increasing temperature (1 °C/min) up to 1050 °C. The resulting materials were finally ball milled in acetone for 5 h and dried at 80 °C. The materials were sieved and particles size of 0.1–0.3 mm was used for all experiments.

2.2. Characterization

The chemical composition of samples were determined by X-ray fluorescence (XRF) using Philips (Panalytical) PW 1480 equipment.

Nitrogen adsorption measurements were carried out at −196 °C with a Micromeritics Tristar system. Prior the adsorption measurements the samples were degassed at 300 °C and 10^{-3} Pa for 24 h. The specific surface areas were calculated according to the Brunauer–Emmet–Teller (BET) method.

The crystal structure of the materials was determined in air with powder X-ray diffraction (XRD) using a Philips PW2050 (X'Pert-APD) diffractometer with Cu K_α radiation (λ = 0.15406 nm). Data were collected varying 2θ between 5° and 75° with a step size of 0.005° and a step time of 1 s.

Temperature programmed reduction (TPR) of the samples was carried out with a home-built set-up, equipped with a TCD detector. First, 40 mg of sample mixed with 40 mg quartz particles were placed in a reactor with a 4 mm inner diameter and heated in a flow of 5%O_2 in He up to 500 °C (10 °C/min) and kept at 500 °C for 1 h. Then the sample was cooled down to room temperature in the same atmosphere. At room temperature the flow was changed to 5%H_2 in Ar and TPR was carried out with a heating rate of 5 °C/min up to 980 °C. The TCD was calibrated *via* reduction of NiO.

2.3. Pulse experiments

Pulse experiments were carried out in a fixed-bed reactor (quartz tube, length 400 mm, internal diameter 2 mm) at 550 °C. About 35 mg of catalyst were packed between two quartz-wool plugs (length approximately 10 mm each). The remaining volume of the reactor was filled with quartz particles, in order to reduce the void space and minimize gas phase reaction. Before each titration test, the catalysts have been pretreated in 10% of O_2 in He flow (20 ml/min, 30 min) at 720 °C in order to remove any trace of water or inorganic compounds physisorbed on surface and keep the catalyst oxygen level as high as possible. The samples were cooled down to reaction temperature under the same atmosphere and gas flow was changed to He (3 ml/min).

After flowing pure He for 15 min, pulses of 300 μl at atmospheric pressure containing 10% C_3H_8 in He were introduced and pulses of a 10% mixture of O_2 in He were used to reoxidize the catalyst, after exposure to C_3H_8 pulses. In all experiments, the regeneration process was confirmed by subsequent propane pulses (not shown here) which always resulted in identical products distribution as compared to fresh material.

The products distributions were monitored by sampling online with a heated capillary to a quadrupole mass spectrometer (Pfeiffer AG Balzers, OmniStar) equipped with Channeltron and Faraday detectors (2–200 amu). Prior to each experiment, the fragment pattern of diluted propane and diluted oxygen were recorded and compared with the fragment pattern of products gas mixture to qualitatively identify the product distribution. Water, propane, oxygen and carbon dioxide were identified monitoring m/z = 18, 29, 32 and 44, respectively, since no other possible products show additional significant contribution to those m/z signals. To determine presence of methane, ethane, ethylene and propylene, two or three m/z signals were monitored for each compound. Because of the similarity in fragmentation patterns and the consequent contribution of several products to the same m/z signal (cross-contamination effect), matrix-type calculation was performed. In this way, formation of CO was also determined *via* m/z = 28, although many compounds as propane, ethylene and carbon dioxide contribute to m/z = 28. These additional contributions were taken into account and subtracted from m/z = 28, resulting in no significant detection of CO but small amount cannot be excluded. Attempt to determine production of H_2 was done by following m/z = 2 but unfortunately negative intensity of that signal was obtained (signal below the MS detection limit) which made the detection of H_2 unreliable. This procedure allows quantitative determination of propane and oxygen conversion only, with an experimental error of about 5%.

As the formation of products could not be quantified, only semi-quantitative comparison of selectivity patterns, called "apparent selectivity", will be reported. The apparent selectivity is based on the integrated area of peaks of the corresponding m/z signals of each compound *versus* time on stream, divided by total integrated areas of all carbon containing products (e.g. for methane: $A(m/z_{CH_4})/A(m/z_{CH_4}) + A(m/z_{C_2H_6}) + A(m/z_{C_2H_4}) + A(m/z_{C_3H_6}) + A(m/z_{CO}) + A(m/z_{CO_2})$). In case of methane, ethane, ethylene and propylene, which were monitored using two or three m/z signals, only the most intense signal was included in the figures.

The possible contribution of gas phase reaction was checked by pulsing propane in the reactor filled with quartz particles only. The conversion of propane was below the detection limit and therefore we can exclude gas phase initiation during the pulse tests.

3. Results and discussion

3.1. Catalyst characterization

3.1.1. Chemical composition and surface area (BET and XRF analysis)

The stoichiometric ratio of metals in the catalyst, measured with XRF analysis, is presented in Table 1 together with surface area values, according to N_2 physisorption.

The observed compositions are in a good agreement with the compositions expected based on the preparation procedures. Assuming specific oxidation state for each metal (La^{3+} and Ni^{2+} for LN and La^{3+}, 90% of Ni^{2+} + 10% of Ni^{3+} and V^{5+} for LNV10) the stoichiometric amount of oxygen can be calculated. The materials have similar, relatively small BET surface areas. This is important for our study because it implies that the diffusion distance between surface and bulk of the oxides is similar. Moreover, the surface areas exposed during the pulse experiments are equivalent. Liu and Au [18] reported a slightly higher value of 9.3 m^2/g for LN, which is probably due to the lower sintering temperature used in that study (800 °C).

The X-ray diffraction patterns obtained for LN and LNV-10 are shown in Fig. 3.

Both LN and LNV10 samples are clearly crystalline and all peaks (except one) were assigned to single K_2NiF_4 tetragonal structure typical for this type of materials [19,20]. The main difference between the two spectra is the change in relative intensity of the main peaks at 2θ = 31.4 and 32.7. These results are very similar to the effect of Cu addition to LN [21]: the K_2NiF_4 structure is retained and the ratio of intensities of the main peaks varies. The reason for the latter observation is not known.

Table 1
Stoichiometric ratio. Properties of mixed oxide catalysts investigated.

Catalyst	Stoichiometric ratio (XRF)			Surface area (m^2/g)
	La	Ni	V	
LN	2.0	1.01	–	2.3 ± 0.2
LNV-05	2.0	0.96	0.05	2.0 ± 0.2
LNV-10	2.0	0.90	0.10	2.0 ± 0.2

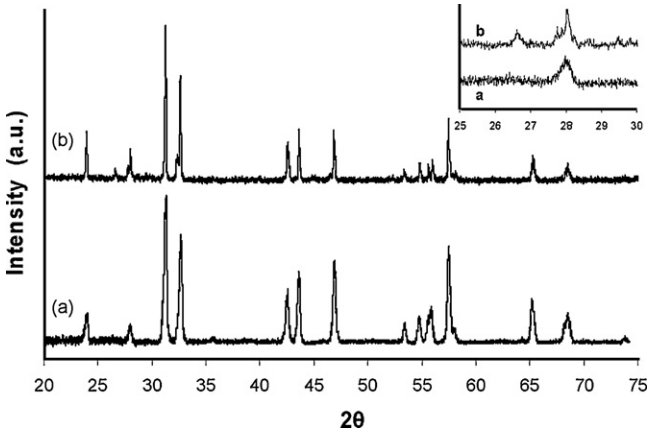

Fig. 3. XRD patterns of fresh LN (a) and fresh LNV-10 (b). XRD pattern in the range $27 < 2\theta < 31$ is shown in the insert.

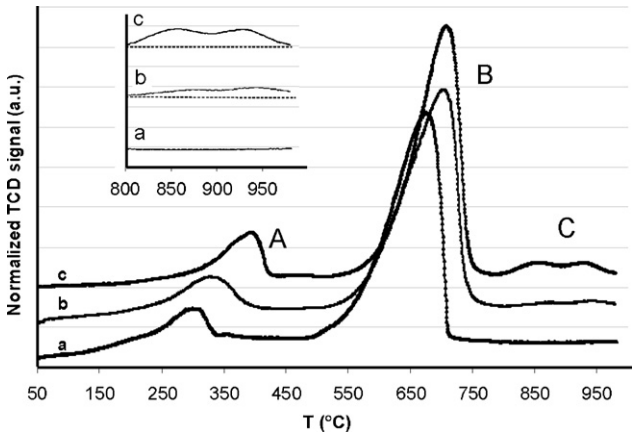

Fig. 4. Temperature programmed reduction on three fresh samples: LN (a), LNV-05 (b) and LNV-10 (c) in H_2 (ramp 50–980 °C). In the insert, TPR profiles at high temperature are highlighted.

An extra peak at $2\theta = 26.6$ was observed in the case of LNV-10 (see Fig. 3, insert). Based on XRD-database [ICDD 2006], this peak cannot be assigned to any of the individual- or mixed oxides possibly present (oxides of La, V and Ni) as well as metallic Ni. The assignment of this peak remains unknown at this time. It should be mention that no contaminants were detected on XRF analysis and only a very small peak related to Mg was present on XPS (not shown here). However, the extra peak at $2\theta = 26.6$ cannot be assigned to Mg, based on XRD-database.

3.1.2. Temperature programmed reduction (TPR)

The TPR profiles of LN, LNV-05 and LNV-10 are shown in Fig. 4.

Two distinctive reduction steps are visible at ~300 and 650 °C for all samples, typical for K_2NiF_4-type of materials. The measured patterns are similar to what has been reported in literature for $La_2NiO_{4+\delta}$ [18,19,22]. In addition, V-doped samples show the presence of a small reduction peak in the temperature interval between 850 and 980 °C (see insert in Fig. 4). As the area of the high temperature peak (peak C in Fig. 4) is proportionally increasing (from 0.09 to 0.20 mmol/g) with the V loading (5% *versus* 10%), this peak is related to reduction of V present in the sample. Based on typical reduction profiles for bulk V_2O_5 in literature [23,24], this peak is assigned to reduction of V^{4+} to V^{3+}.

Table 2 presents a quantitative evaluation of the TPR profiles shown in Fig. 4. The first reduction step (peaks A in Fig. 4) of LN corresponds to removal of 0.37 mmol O per gram (see Table 2). Saez Puche et al. [25] assigned the low temperature reduction of $La_2NiO_{4+\delta}$ to removal of over-stoichiometric oxygen, related to the presence of Ni^{3+}, based on electron diffraction patterns and TGA analysis. Therefore, we also assign the low temperature peak in TPR to removal of over-stoichiometric oxygen and reduction of Ni^{3+} to Ni^{2+}. Consequently, the initial composition of the material (at room temperature) is $La_2NiO_{4.15}$. This is in good agreement with results of Bassat et al. [26], who reported comparable composition ($La_2NiO_{4.16}$) based on TGA data under identical reductive atmosphere.

The amount of atomic oxygen removed from the LN sample during the reduction around 650 °C (see Table 2), as calculated based on the amount of molecular H_2 consumed, was 2.5 mmol/g, which is in a good agreement with complete reduction of Ni^{2+} to Ni^0. After this reduction step, the final composition of the material is $Ni^0 + La_2O_3$, in full agreement with literature [22] and confirmed with XRD measurements (not shown). No further reduction at temperatures higher than 750 °C was observed for $La_2NiO_{4+\delta}$.

Addition of V causes the low temperature reduction peak to shift to higher temperature as compared to LN (Fig. 4b and c). The onset and offset temperature of the first peak was shifted up by 30 and 60 °C for the LNV-05 and LNV-10, respectively (Table 2).

It has been reported [16,27] that the insertion of Sr as dopant in a K_2NiF_4-type oxide (Pr_2CoO_4 and Eu_2NiO_4) affects the reduction profile of the materials, in agreement with our observation.

The fact that the low temperature reduction peak is shifted to higher temperature with increase in V loading is additional evidence that the low temperature peak is related to over-stoichiometric oxygen. If this peak would have been due to reduction of amorphous NiO, as proposed in literature [22,28], no shift in temperature would be expected, because it is not reasonable to assume that the reducibility of a separate amorphous NiO phase would be influenced by the presence of vanadium.

The presence of V also stabilizes the mixed oxide regarding reduction to Ni^0 (reduction peak B in Fig. 4) whereas the onset temperature is slightly shifted to higher value. Surprisingly, experimentally observed amounts of oxygen removed for LNV-05 and LNV-10 (2.47 and 2.42 mmol/g, respectively – B peak, Table 2) are higher than theoretical values assuming complete reduction of Ni^{2+}, which would result in 2.37 and 2.25 mmol/g, respectively. This difference may be caused by an additional contribution due to the reduction of V (V^{5+} to V^{4+}), which was reported to occur at 650–700 °C for bulk V_2O_5 [23,24].

3.2. Pulse experiments

3.2.1. LN

The propane conversion over LN during pulse experiments at 550 °C is shown in Fig. 5.

The conversion gradually decreased during the first 13 pulses of propane from 40% at the first pulse to below 5% from the 8th pulse onwards, which is due to consumption of oxygen in the oxide. The conversion suddenly increased to ~50% when continuing pulsing with propane.

The product distribution when pulsing propane over $La_2NiO_{4+\delta}$ at 550 °C, as well as the re-oxidation of the catalyst by pulsing O_2, are shown in Fig. 6. CO_2 and H_2O are observed as main products when pulsing propane over freshly oxidized material, indicating deep oxidation with oxygen provided by $La_2NiO_{4+\delta}$ (Eq. (1)).

$$C_3H_8 + 10O_{CAT.} \Rightarrow 3CO_2 + 4H_2O \quad (1)$$

where $O_{CAT.}$ indicates the oxygen released from the catalyst.

The products mixture contains also CH_4, C_2H_4 and C_3H_6, demonstrating that both cracking as well as dehydrogenation reactions

Table 2
Quantification from TPR. Temperature range where the reductions occurs and amount of oxygen removed per gram of fresh material.

Catalyst	Peak A			Peak B			Peak C		
	Onset T (°C)	Offset T (°C)	Removed oxygen (mmol/g)	Onset T (°C)	Offset T (°C)	Removed oxygen (mmol/g)	Onset T (°C)	Offset T (°C)	Removed oxygen (mmol/g)
LN	132 ± 10	379 ± 20	0.37 ± 0.02	498 ± 20	725 ± 15	2.50 ± 0.1	–	–	–
LNV-05	165 ± 15	410 ± 20	0.40 ± 0.02	525 ± 20	765 ± 15	2.47 ± 0.1	790 ± 20	Until end	0.09 ± 0.01
LNV-10	207 ± 20	436 ± 20	0.42 ± 0.02	545 ± 20	775 ± 15	2.42 ± 0.1	800 ± 15	Until end	0.20 ± 0.01

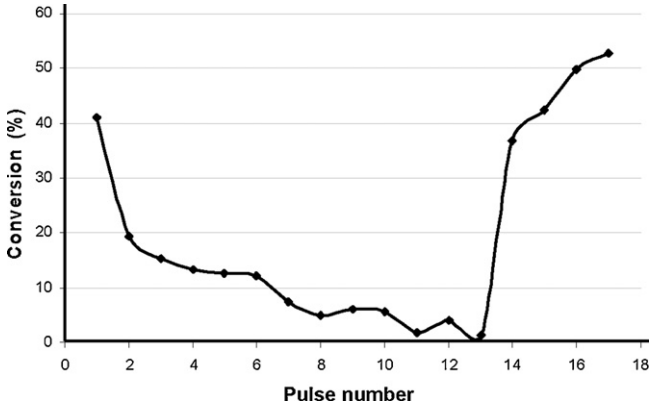

Fig. 5. Propane conversion profile during the titration test on $La_2NiO_{4+\delta}$ at 550 °C. Carrier gas (He) flow rate, 3 ml/min; propane pulses, 10% C_3H_8 in He; sampling loop for pulsing, 300 μl.

contribute (Eqs. (2)–(4)).

$$C_3H_8 + O_{CAT.} \Rightarrow CH_4 + C_2H_4 + O_{CAT.} \quad (2)$$

$$C_3H_8 + O_{CAT.} \Rightarrow C_3H_6 + H_2 + O_{CAT.} \quad (3)$$

$$C_3H_8 + O_{CAT.} \Rightarrow C_3H_6 + H_2O \quad (4)$$

The formation of C_3H_6 may be explained by selective dehydrogenation of propane with formation of H_2 (Eq. (3)) or by oxidative dehydrogenation of propane, forming water (Eq. (4)). Probably oxidative dehydrogenation contributes since H_2O was always detected; however we cannot rule out formation of H_2O *via* oxidation of H_2. The contribution of dehydrogenation remains unclear since H_2 could not be monitored. It should be mentioned that the formed C_3H_6 might be further converted to deep oxidation products since at the reaction temperature used (550 °C) olefins possess higher reactivity in oxidation reaction than paraffins [29].

The CO_2 production diminished rapidly with the number of pulses (Fig. 6) and decreased below the detection limit after 7th pulse, while formation of propylene was approximately constant, thus increasing the selectivity towards propylene.

After pulse 12 the products distribution changed with a sudden increase in propane conversion. No C_3H_6, C_2H_4 and H_2O were observed at this stage, instead only CO and CH_4 were observed. Additionally, coke was deposited on the catalyst surface, as will be discussed in more detail below. After the titration test, the catalyst was regenerated by pulsing oxygen (Fig. 6, right hand side). The pulses 1–4 resulted in complete oxygen consumption and formation of CO_2, testifying that carbon was deposited on catalyst surface. O_2 level reached a plateau value, equal to blank O_2 pulses, after pulse 6, indicating complete regeneration of the samples. However, no CO_2 was detected during regeneration by pulsing oxygen after exposing the sample to only 11 pulses of propane. Therefore, carbon deposition took place exclusively after the drastic change in selectivity and the sudden increase of propane conversion level. We suggest that at this moment Ni^{2+} starts to reduce to Ni metal, forming CO and CH_4 according to Eq. (5) (overall equation); it is important to note that the ratio of intensities of CO and CH_4 in Fig. 6 cannot be compared quantitatively. Ni metal is well known to easily form coke deposits as well as carbon nanofibers [30].

$$La_2NiO_4 + C_3H_8 \rightarrow Ni^0 + CO + 2CH_4 + La_2O_3 \quad (5)$$

The total amount of atomic oxygen consumed during regeneration, involving both catalyst reoxidation and carbon combustion, is 0.180 mmol/g, while regeneration after only 11 pulses of propane consumed 0.140 mmol/g oxygen only. Therefore it is affirmed here that 0.14 mmol/g of oxygen was needed to reoxidize the catalyst and 0.04 mmol/g oxygen is consumed by carbon combustion, CO formation and reoxidation of Ni metal.

To conclude, propane conversion shifted from deep oxidation to reasonable selectivity towards olefins when varying the amount and consequently the reactivity of over-stoichiometric oxygen species. Further removing of oxygen causes initiation of another reaction pathway, forming CO, CH_4 and coke, which is probably due to Ni^0 formation.

3.2.2. LNV

Doping LN with vanadium does not affect drastically the conversion trend at the initial stage of the pulse experiment (Fig. 7), as compared to Fig. 5. The activity of the materials diminished with the number of pulses for all materials. Within the first 10 pulses LN showed higher propane conversion than V-doped LN, denoting the higher reactivity of oxygen ion species. Figs. 8 and 9 show the product distributions during pulsing propane at 550 °C over LNV-05 and LNV-10, respectively, as well as the re-oxidation of the catalyst by pulsing O_2.

Initially, the product distribution was similar to un-doped LN catalyst: main products were CO_2 and H_2O (deep oxidation, Eq. (1)). Similar to un-doped catalyst, the catalyst was depleted in oxygen during pulsing propane, decreasing the catalyst oxidation degree as well as the propane conversion. Continuing pulsing, the V-doped catalysts showed a constant production of propylene (Eqs. (3) and (4)), probably due to the decrease of chemical potential of remaining oxygen in the slightly reduced catalyst. Also cracking products (CH_4 and C_2H_4) were constantly produced (Eq. (2)). In the case of

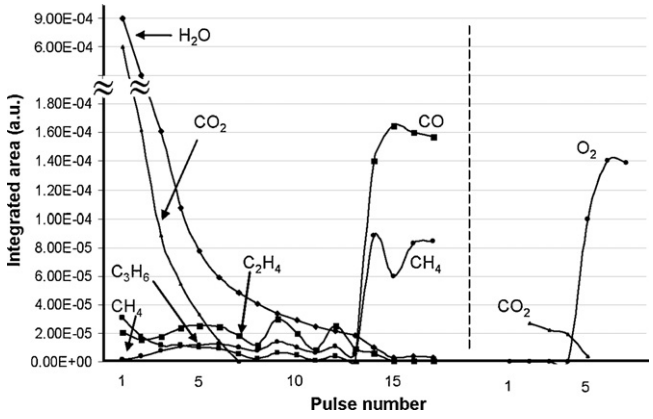

Fig. 6. Products distribution during the titration test on $La_2NiO_{4+\delta}$ at 550 °C (left hand side) and regeneration profile of the catalyst by O_2 pulse (right hand side). Carrier gas (He) flow rate, 3 ml/min; propane pulses, 10% C_3H_8 in He; oxygen pulses, 10% O_2 in He; sampling loop for pulsing, 300 μl.

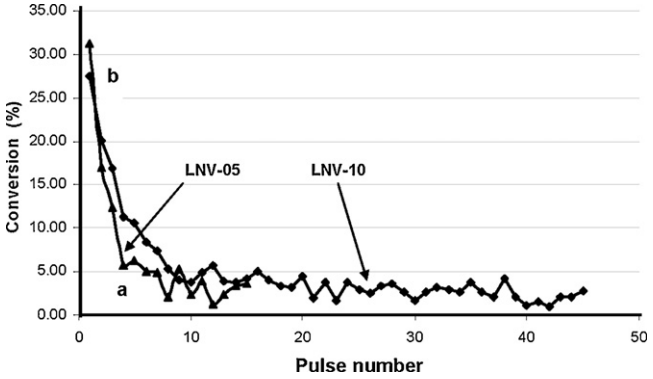

Fig. 7. Propane conversion profiles during the titration tests on $La_2Ni_{0.95}V_{0.05}O_{4+\delta}$ (a) and $La_2Ni_{0.9}V_{0.1}O_{4+\delta}$ (b) at 550 °C. Carrier gas (He) flow rate, 3 ml/min; propane pulses, 10% C_3H_8 in He; sampling loop for pulsing, 300 μl.

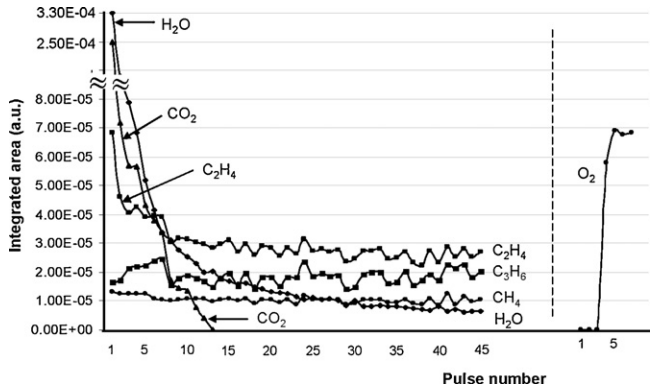

Fig. 8. Products distribution during titration test (45 pulses) of $La_2Ni_{0.9}V_{0.1}O_{4+\delta}$ at 550 °C (left hand side) and regeneration profile of the catalyst by O_2 pulse (right hand side). Carrier gas (He) flow rate, 3 ml/min; propane pulses, 10% C_3H_8 in He; oxygen pulses, 10% O_2 in He; sampling loop for pulsing, 300 μl.

LNV-05 (up to 15 pulses of propane) and LNV-10 (up to 45 pulses of propane) no drastic increase in conversion and sudden change in product distribution were noticed when continuing pulsing, in contrast to LN. Stable performance was maintained in a much broader window of pulses as compared to LN.

The amounts of oxygen consumed during the regeneration processes after comparable number of propane pulses (15 pulses for LNV-05 and LNV-10, 11 pulses for LN) were quantified: 0.106 mmol/g for LNV-10, 0.110 mmol/g for LNV-05 and 0.140 mmol/g for LN, which is the highest value despite the lower number of pulses. These results reveal that less oxygen is removed during propane pulses with increasing V content, in agreement with the TPR result in Fig. 4. The stabilizing effect of V therefore does not depend on the reducing agent used, hydrogen or propane.

The apparent selectivity of olefins is shown in Fig. 10.

Unfortunately, the selectivity could not be calculated quantitatively since the product distribution was analyzed by MS without a full calibration. The apparent selectivity to olefin was lower than 40% during first three pulses for all three catalysts, due to mainly CO_2 formation. It is clear that especially LN produced much CO_2 initially, which in agreement with the observation that more oxygen is being removed from LN as compared to the V-containing catalysts. Continuing pulsing propane and reducing the catalyst, V-doped LN showed an increase of apparent selectivity to olefin up to constant value (80%) for around 30 pulses while it suddenly decreased below

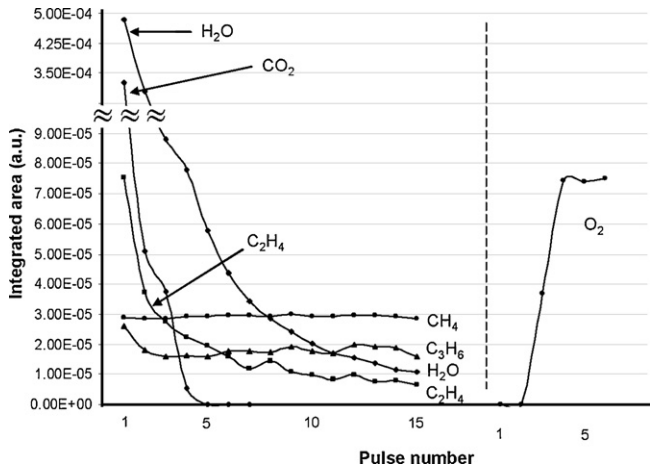

Fig. 9. Products distribution during titration test (15 pulses) of $La_2Ni_{0.95}V_{0.05}O_{4+\delta}$ at 550 °C (left hand side) and regeneration profile of the catalyst by O_2 pulse (right hand side). Carrier gas (He) flow rate, 3 ml/min; propane pulses, 10% C_3H_8 in He; oxygen pulses, 10% O_2 in He; sampling loop for pulsing, 300 μl.

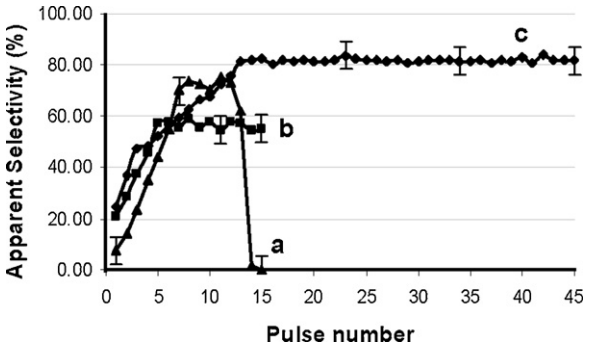

Fig. 10. Apparent olefins ($C_2H_4 + C_3H_6$) selectivities during titration tests on LN (a), LNV-05 (b) and LNV-10 (c). Only few error margin bars are shown in the figure as they are constant (±5%) for the three different samples. Carrier gas (He) flow rate, 3 ml/min; propane pulses, 10% C_3H_8 in He; sampling loop for pulsing, 300 μl.

the detection limit for LN. LNV-05 also showed constant apparent selectivity to olefin within 15 pulses (not tested further). It is obvious that all three catalysts result in significant selectivity to olefins when operated at optimal reduction degree. It is important to note that the propane conversion levels are comparable and low (typically 4%) under these conditions for all three catalysts. Therefore, the small, though significant, differences in olefin selectivity between the three catalysts (LNV-10 > LN > LNV-05) must be due to differences in the ratios between the rate of activation of propane *versus* the rate of activation of olefins for the three catalysts.

Therefore we conclude that vanadium contributes on reducing the activity of oxygen species, reducing the amount of CO_2 formed (comparison of Figs. 6 and 8), consequently reducing the amount of oxygen consumed, enhancing the selectivity towards olefins. 10% V as dopant in LN is required to achieve the highest yields to olefins.

Contrary to what observed for LN, during the regeneration by pulsing oxygen (Figs. 8 and 9, right hand side) after the titration test, no CO_2 formation was observed, denoting no carbon deposition during propane pulses. This observation confirms that the presence of V prevents formation of metallic Ni within the window of operation in this study.

4. Conclusions

It was shown that over the oxidized materials, too high activity of oxygen species was responsible for formation of deep oxidation products (CO_2 and H_2O) for both doped and un-doped materials. The scenario changed after partial removal of oxygen and consequent decrease of reactivity of the remaining oxygen species: C_3H_6, C_2H_4, CH_4 and H_2O were the only products detected with beneficial effect on selectivity to olefins.

The presence of vanadium as dopant in LN enhances the material stability towards reduction in H_2. The stabilization of over-stoichiometric oxygen positively affected the products distribution in pulse experiment, as less CO_2 was produced (and less oxygen consumed), over deep-oxidized catalyst. Also the stability of lattice oxygen, bonded to Ni atoms, was influenced by the dopant. It was shown that the presence of V delayed the release of lattice oxygen and the consequent formation on Ni^0, responsible for drastic detrimental change in reaction patterns (CO, CH_4 and coke as products). Therefore, the V-doped catalyst showed much larger window (more than 30 propane pulses) in which the selectivity towards propylene was constant and promising, contrary to un-doped catalyst.

Slightly reduced V-doped LN is a promising material for selective oxidation of propane if a specific reduction level of the catalyst can be maintained during the process; e.g. by operating a cat-

alytic dense membrane reactor with well balanced oxygen diffusion *versus* oxygen consumption at the propane side. LNV-10 is probably the best candidate as it showed the better selectivity towards propylene.

Acknowledgements

The authors would like to thank Dr. B.L. Mojet and Dr. C. Trionfetti for inspiring discussions as well as precious help on writing this paper. We thank ACTS/NWO, The Netherlands for financial support (project number 053.62.004).

References

[1] I.M. Dahl, K. Grande, K.J. Jens, E. Rytter, A. Slagtern, Appl. Catal. 77 (1991) 163–174.
[2] C. Mazzocchia, C. Aboumard, D. Diagne, E. Temesti, J.M. Herrmann, G. Thomas, Catal. Lett. 10 (1991) 181–192.
[3] A. Cherrak, R. Hubaut, Y. Barbaux, G. Mairesse, Catal. Lett. 15 (1992) 377–383.
[4] R.H.H. Smits, K. Seshan, H. Leemreize, J.R.H. Ross, Catal. Today 16 (1993) 513–523.
[5] M.C. Kung, H.H. Kung, J. Catal. 134 (1992) 668–677.
[6] R.M. Contractor, H.E. Bergna, H.S. Horowitz, C.M. Blackstone, B. Malone, C.C. Torardi, B. Griffeths, U. Chowdhry, A.W. Sleight, Catal. Today 1 (1987) 49–58.
[7] S. Haag, A.C. van Veen, C. Mirodatos, Catal. Today 127 (2007) 157–164.
[8] P.J. Gellings, H.J.M. Bouwmeester, in: P.J. Gellings, H.J.M. Bouwmeester (Eds.), The CRC Handbook of Solid State Electrochemistry, first ed., CRC Inc., 1997, p. 520.
[9] H. Fjellvag, O.H. Hansteen, B.G. Tilset, A. Olafsen, N. Sakai, H. Seim, Thermochim. Acta 256 (1995) 75–89.
[10] R. Chiba, F. Yoshimura, Y. Sakurai, Solid State Ionics 124 (1999) 281–288.
[11] E.V. Tsipis, E.N. Naumovich, A.L. Shaula, M.V. Patrakeev, J.C. Waerenborgh, V.V. Kharton, Solid State Ionics 179 (2008) 57–60.
[12] L. Minervini, R.W. Grimes, J.A. Kilner, K.E. Sickafus, J. Mater. Chem. 10 (2000) 2349–2354.
[13] C. Li, T. Hu, H. Zhang, Y. Chen, J. Jin, N. Yang, J. Membr. Sci. 226 (2003) 1–7.
[14] E.V. Tsipis, E.A. Kiselev, V.A. Kolotygin, J.C. Waerenborgh, V.A. Cherepanov, V.V. Kharton, Solid State Ionics 179 (2008) 2170–2180.
[15] S. Miyoshi, T. Furuno, O. Sangoanruang, H. Matsumoto, T. Ishihara, J. Electrochem. Soc. 154 (2007) B57–B62.
[16] L. Hui, C. Ping, G. Yuping, L. Yueqing, L. Guanglie, X. Yuanzhe, M. Futai, J. Solid State Chem. 141 (1998) 99–104.
[17] R.H.E. van Doorn, H. Kruidhof, A. Nijmeijer, L. Winnubst, A.J. Burggraaf, J. Mater. Chem. 8 (9) (1998) 2109–2112.
[18] B.S. Liu, C.T. Au, Appl. Catal. A 244 (2003) 181–195.
[19] B.S. Liu, C.T. Au, Catal. Lett. 85 (2003) 165–169.
[20] D.E. Rice, D.J. Buttrey, J. Solid State Chem. 105 (1993) 197–210.
[21] T.C. Vaimakis, Thermochim. Acta 206 (1992) 219–234.
[22] G.S. Gallego, F. Mondragon, J. Barrault, J.M. Tatibouet, C. Batiot-Dupeyrat, Appl. Catal. A 311 (2006) 164–171.
[23] M.M. Koranne, J.G. Goodwin, G. Marcelin, J. Catal. 148 (1994) 369–377.
[24] H. Bosch, B.J. Kip, J.G. van Ommen, P.J. Gellings, J. Chem. Soc. Faraday Trans. 80 (1984) 2479.
[25] R. Saez Puche, J.L. Rodriguez, F. Fernandez, Inorg. Chem. Acta 140 (1987) 151–153.
[26] J.M. Bassat, P. Odier, J.P. Loup, J. Solid State Chem. 110 (1994) 124–135.
[27] H. Zhong, X. Zeng, Kinet. Catal. 47 (2007) 423–429.
[28] E. Ruckenstein, Y.H. Hu, J. Catal. 161 (1996) 55–61.
[29] A. Lofberg, C. Pirovano, M.C. Steil, R.N. Vannier, E. Bordes-Richard, Catal. Today 112 (2006) 8–11.
[30] K.P. De Jong, J.W. Geus, Catal. Rev. Sci. Eng. 42 (2000) 481–510.